Myriam Kaiser, Hamza Dounassre, Max Kahmann, Julian Hellstern, Jonas Kleiner, Christoph Tillkorn, and Daniel Flamm, "Chamfered-edge laser cleaving of transparent materials", Proc. SPIE 11991, Frontiers in Ultrafast Optics: Biomedical, Scientific, and Industrial Applications XXII, 1199107 (4 March 2022); https://doi.org/10.1117/12.2607604.

Chamfered-edge laser cleaving of transparent materials

Myriam Kaiser,[a] Hamza Dounassre,[a] Max Kahmann,[a] Julian Hellstern,[b] Jonas Kleiner,[a] Christoph Tillkorn,[b] and Daniel Flamm[a]

[a]TRUMPF Laser- und Systemtechnik GmbH, Johann-Maus-Str. 2, 71254 Ditzingen, Germany
[b]TRUMPF Laser GmbH, Aichhalder Str. 39, 78713 Schramberg, Germany

ABSTRACT

We report on the separation of glass substrates with customized edge contours including C-shapes. To achieve single-pass laser modifications along the entire contour geometry a processing optics is presented where a multitude of foci are simultaneously distributed inside a specific volume using a large-working-volume focusing unit. Tangential angles of the focus trajectory to the surface can be almost arbitrarily chosen and amount to even less than 45-deg in case of aiming for chamfered edges. After having induced laser modifications along the desired edge geometry, separation is done chemically in the present case. The glass articles, thus fabricated, meet the demands of the display industry in terms of bending strength and surface quality.

Keywords: Beam shaping, ultrafast optics, laser materials processing, digital holography, structured light

1. INTRODUCTION

Concepts for ultrafast laser cutting of sheet-like transparent materials were successfully transferred to industry within recent years. Flexible ultrashort pulsed laser systems are available as well as adapted optical heads providing customized non-diffracting beams for single-pass, full-thickness operations with > m/s-feed rates.[1,2] The fabricated substrates with straight face-edges, see schematic in Fig. 1 (a), are susceptible to chipping and cracking in the event of an impact as stress is accumulated at the 90-deg corners. Substrates with reduced tangential edge angles α, as known from chamfered, beveled or C-shaped edges, will exhibit higher bending stabilities in case of impacts, see Fig. 1 (b)–(d).[3–5]

If a glass substrate is cut to size, various further process steps are required, such as hardening, polishing, cleaning, etc. The longer and more complex the further processing of a substrate, the more likely it is that defects will be introduced. Here, a shaped glass edge will be very effective in protecting the substrate from cracks, too. Chamfering is, thus, highly desired immediately during the first process steps. Laser-based processing becomes highly attractive when cutting and chamfering can be performed in a single machining step.[5]

We report on holographic 3D-beam splitting concepts that, in combination with ultrashort laser pulses, allow to deposit energy in the volume of transparent materials along arbitrary edge geometries in a single pass.[6,7] Associated tangential angles to the surface can be almost arbitrarily chosen and amount to even less than 45-deg.[5] The laser modification step is followed by the separation step, which is performed by chemical etching in the present case.[5,8] Equally conceivable are mechanical or thermal separation strategies.[9] The generated glass articles with shaped edges convince with high surface qualities and bending strengths comparable to conventional straight-cut substrates.[5]

The processing optics operates under vertical incidence and requires single-side access to the workpiece only. The ability to introduce volume modifications along the entire substrate edge geometry within a single pass allows for laser processing in the order of one m/s.[5]

In addition to the important motive of protecting the glass edge with a chamfer, the technology presented enables the production of edge geometries that improve the mounting of optical components. In this case, special edge contours—usually mechanically polished—allow flush closing or self-centering,[10,11] see schematics in Fig. 1 (e)–(f). To this end, focus distributions and manufactured customized edges are presented in the following,

Further author information:
E-Mail: daniel.flamm@trumpf.com.

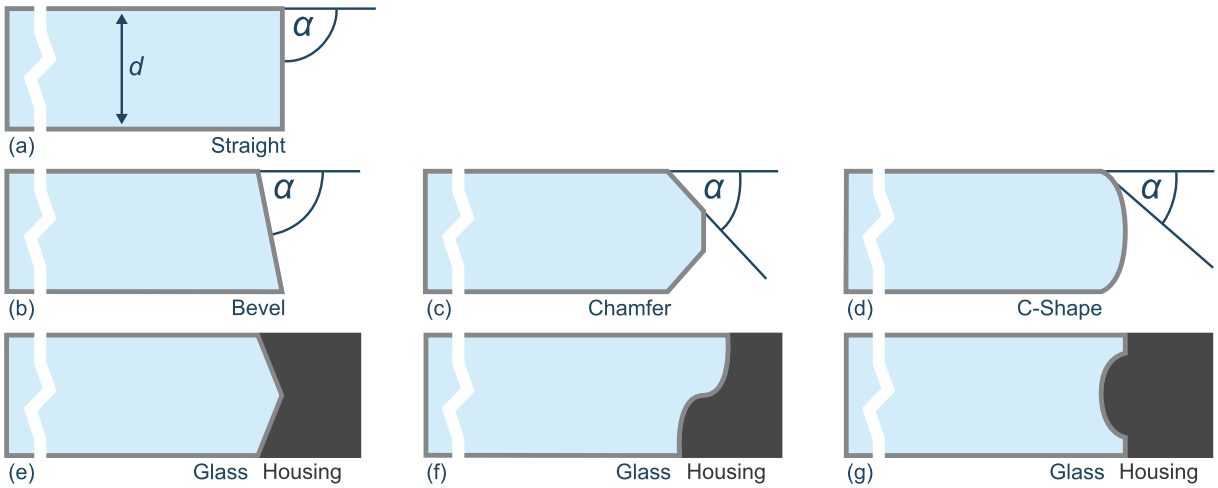

Figure 1. Tailored-edge glass contours for different applications. Straight face edge and definition of local or global tangential edge angle to the surface α (a). Beveled (b), chamfered (c), and C-shaped (d) edge for substrate protecting purpose.[5] Profiles in apex (e), step (f), and half-circle (g) shape for substrate mounting and auto-centering applications.

showing that our concept enables completely new degrees of freedom for mounting strategies of substrates or optics.

The paper is organized as follows. With the following two sections, we will shed light on the two main components that make the procedure possible. These are the holographic beam splitter (Sec. 2) as well as the focusing unit (Sec. 3) that generates diffraction-limited focuses in a large working volume. We will finally present samples that fulfill our motivation and discuss their quality (Sec. 4).

2. HOLOGRAPHIC 3D-BEAM SPLITTERS

Recently, we demonstrated the beneficial use of holographic 3D-beam splitters for controlled energy deposition in a sub-millimeter scaled working volume.[5–7] The concept is used to split a number of focus copies along a desired trajectory that fits to the shape of the substrate's edge. These beam splitters applied to ultrafast laser radiation enable to process the transparent material and to generate different types of volume modifications.[12] Depending on the exact type of light-material interaction, modifications are generated that, for example, result in a weakening of the material or that exhibit an increased selective etchability. Accordingly, different separation strategies can be employed, such as the application of mechanical[1] or thermal stress,[9] or the use of a chemical etching bath.[13,14] Typically, for glass cutting purposes, type–III–regime modifications[12]—so called voids caused by microexplosions—are to be aimed, requiring a precise control of peak intensities in a spatially confined focus zone.[15] For the simultaneous generation of voids, or void chains, along a desired edge contour, ideally, a single contiguous intensity distribution is shaped along the desired geometry which is able to modify the substrate within a single pass. Elongated and curved focus distributions are common to the structured light community, see, for example the famous Airy beam[16] or non-diffracting beams propagating along accelerating trajectories.[17] However, as discussed and geometrically deduced in Ref. 5, intensity distributions with small radii of curvatures or local 45-deg tangential angles require an enormous effort for the focusing unit as associated NAs approaches 1. This is confirmed by recent Airy-beam-based glass-cutting experiments reaching $\alpha \approx 70°$,[18,19] cf. Fig. 1. Furthermore, we are looking for an optical solution that is also applicable in an industrial environment. This means that the optical head should not be inclined and also that a working distance of a few millimeters should be maintained during processing.[2,6]

As mentioned in the beginning, our laser optical solution to these "industrial" demands, makes use of multiple volume-split foci. Although we pursue a beam splitting concept, we refer to the entirety of the foci as *one* focus distribution. This is due to the fact that simultaneity in the introduction of the material modifications is decisive for the process presented. It is the simultaneous impact of focus set to the material that generates connected modifications without shielding effects which, in turn, enables the substrate separation in the first place.[7]

Following the edge contour examples depicted in Fig. 1 and discussed in Sec. 1, we demonstrate useful 3D-focus distributions in Fig. 2, generated with holographic phase-only beam splitters. Such diffractive optical elements are common to the materials processing community that allow for parallel processing for, e.g., drilling or ablation applications.[20] Usually, foci are split in a single propagation plane (2D-beam splitting)[21]—often combined with optical scanners.[6] The expansion to the third spatial dimension, see z-axes, thus 3D-beam splitting, is a technique successfully used for parallel micromanipulation,[22] multifocal microscopy,[22] optical data storage,[23] and for micromachining the volume of transparent materials (ultrafast laser writing[24] and welding[6]). For $2f$-like configurations, as used in this work, the design algorithm and the experimental verification is provided in Refs. 7 and 6, respectively. Here, holographic tilt and defocus transmission functions[25] are multiplexed (one for each spot to be split) with well-defined phase relations resulting in particularly efficient and homogeneous focus distributions.[7] The final phase-only hologram can be displayed by a flexible liquid-crystal-on-silicon-based spatial light modulator (SLM) or realized by a static diffractive optical element.[5] In the examples depicted in Fig. 2, we intendedly omit clear length specifications, as number of spots and their density and dimensions need to be adapted to the material and the separation strategy. However, the z-dimensions for the first and last spot may equal typical display glass thicknesses of about $\sim 0.5\,\mathrm{mm}$. As can be seen in the examples, intensity distributions follow, for example, beveled [Fig. 2 (b)] or chamfered [Fig. 2 (c)] edges. Equally conceivable are apex [Fig. 2 (e)] or half-circle shapes [Fig. 2 (g)]. Although the focal distributions, i.e. the entirety of the beam-split foci, may be arranged along accelerated trajectories, including such cases where local tangential angles to the surface amount to 45-deg,[2,5] the individual Gaussian foci still propagate parallel to the optical axis, cf. Fig. 2. At first glance, this situation is unfavorable for material processing, since we expect elongated modifications aligned along this axis,[26,27] which, depending on the edge contour, will extend into the useful part of the workpiece.[5] We will clarify this notoriously complex situation experimentally by analyzing the laser-induced modifications in Sec. 4 and by applying a selective etching strategy for the actual separation.[5]

From a laser-optical perspective the presented structured light concept makes a wide range of applications conceivable and is not restricted to the micro-machining of transparent materials. The broad accessibility of liquid-crystal-on-silicon based SLMs that may act as flexible 3D-beam splitter, allow the iterative optimization[6] of focus distributions for a respective application or, considering the tailored-edge purpose of this work, substrate shape and can also be combined with *in situ* diagnostics.[14,28,29] The spatial resolution of commercially available SLMs such as the Hamamatsu X15223 series with pixels of $12.5\,\mu\mathrm{m}$ pitch enables to split into several hundred spots. Here, Fig. 2 shows only a small selection of the beam splitting possibilities. If stationary phase-only diffractive optical elements (DOEs)[6,7] are used the number of volume-split spots could easily be increased to more than 1000. Here, the numerical effort for optimizing the homogeneity of the spot set and for reducing the power in unwanted diffraction orders represents the main limiting factor.

3. LARGE-WORKING-VOLUME MICROSCOPE OBJECTIVES

In the previous section, we discussed the fundamentals of simultaneously generating a large number of spots in a given working volume along a desired edge geometry. In order to cope with the high numerical effort in the wave-optical hologram design,[7] we use *ideal* optical components in thin element approximation as well as far-field operators and the angular spectrum method.[30] Now, of course, the question remains whether a *real* focusing unit is at all capable of providing diffraction-limited foci in the required working volume. Ideally the spot distribution's high level of uniformity, cf. Fig. 2, is not altered by the real focusing and the single spots exhibit radial symmetric intensity profiles (no preferential direction). Furthermore, we are aiming for an industrially suitable machining concept in which the focusing unit efficiently provides the focus shape with a considerable working distance and is able to resist millijoule-class ultrashort pulses.[5]

Although our process is not limited to this, here, we focus on processing of display glasses that measure $d \approx 0.5\,\mathrm{mm}$ in thickness, cf. Sec. 2, and, thus require a working volume of $V \approx d^3$. Following the efficient cutting of display glasses with non-diffracting beams (straight face edges),[1,31,32] we aim for focus diameters in the range of $(1 \ldots 5)\ \mu\mathrm{m}$. The focusing device should therefore feature a numerical aperture of $\mathrm{NA} \gtrsim 0.2$ and an effective focal length of $f_{\mathrm{eff}} \lesssim 20\,\mathrm{mm}$

As mentioned before, the requirements on the imaging performance of the microscope lenses are high as aberrations within the comparatively large working volume should be negligibly small. In practice, however, a

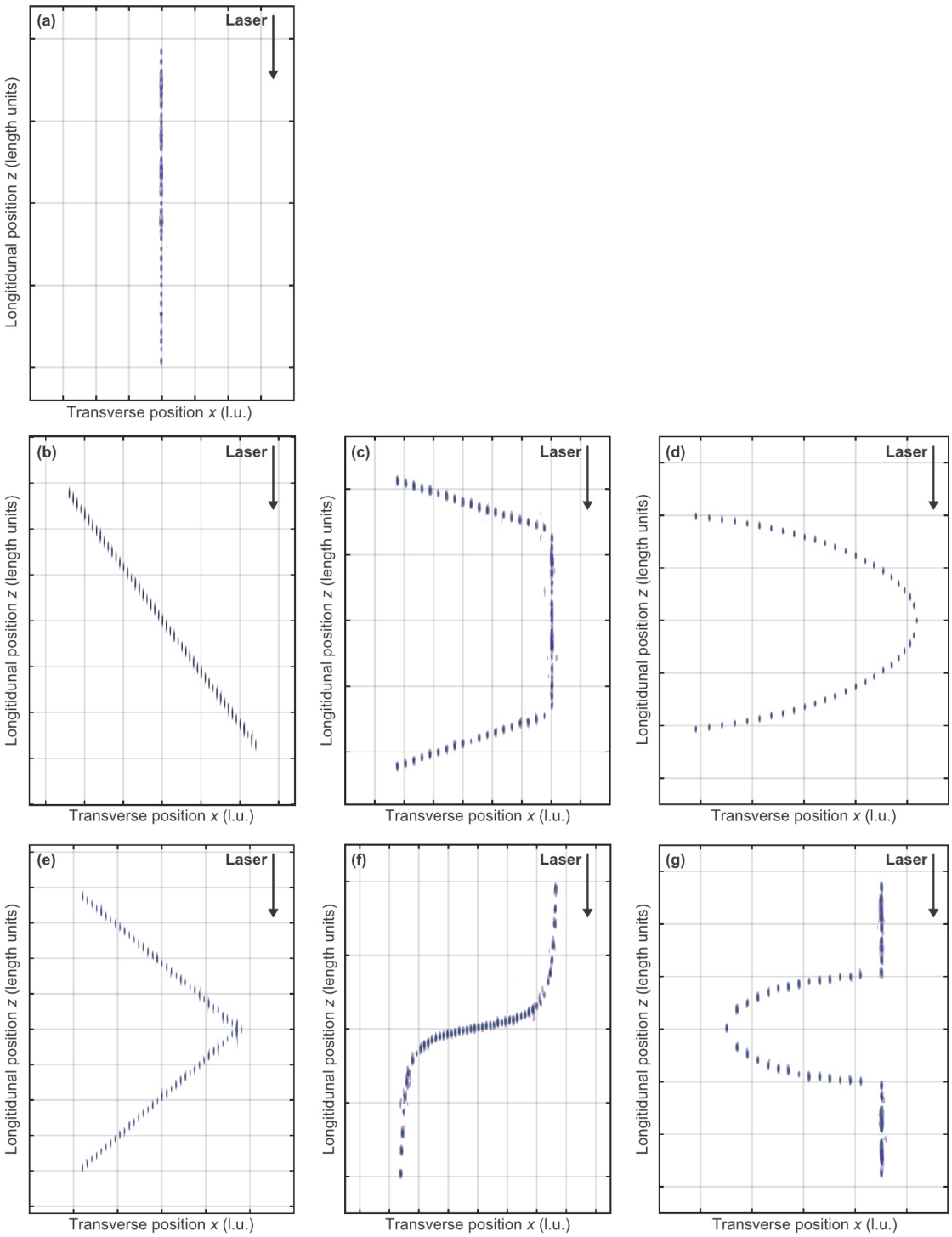

Figure 2. Following the seven edge geometry examples shown in Fig. 1, a menu of 3D-focus distributions useful for tailored edge cleaving is presented. In each case, the z-axis corresponds to the propagation direction. Length dimensions not shown on purpose. Each focus distribution can be adapted to the substrate thickness, typically $\sim 0.5\,\mathrm{mm}$. For the sake of clarity, the spots are weighted equally. Depending on the material, edge geometry and separation strategy, an adapted weighting is reasonable and possible.

large axial and lateral working volume lead to an inherent physical limitation and conflict at high numerical apertures. An absence of lateral aberrations requires the system to satisfy the Abbe sine condition.[33] Hence residual spherical aberrations will occur over the axial range. On the other hand, the absence of axial aberrations requires the Herschel condition to be satisfied resulting in remaining lateral aberrations mainly composed by coma.[33] In particular, the rotational symmetry of the individual foci is important for a controlled laser modification process.* Therefore, the microscope lenses have been designed to satisfy the sine condition with residual spherical aberrations along the axial range.

In order to demonstrate the absolute need for a multi-lens focusing objective when processing large volumes with NAs above 0.2, ray- and wave-optical simulations have been conducted depicted in the scenario of Fig. 3. Here, the performance of a microscope objective (six lenses and cover glass) (top) and a conventional (single lens) asphere (bottom) can be directly compared. The simple optical setup mainly consists of the beam splitter and the focusing unit in a $2f$-like configuration,[5] represented by black boxes on the left hand side. For the tailored-edge processing of display glasses, a working volume is aimed with $V \approx (500\,\mu\mathrm{m})^3$. For this reason, we investigate three focusing scenarios, where three spots are distributed at following coordinates within the processing volume: $(y = -250\,\mu\mathrm{m}, z = -250\,\mu\mathrm{m})$, $(y = 0\,, z = 0\,)$, and $(y = 250\,\mu\mathrm{m}, z = 250\,\mu\mathrm{m})$. Here, the focus at $(y = 0\,, z = 0\,)$ is positioned at the geometrical focus of the focusing units acting as reference. For the sake of simplicity, we keep the distribution of the spots at two dimensions and set $x = 0$ for all three cases. The ray- and wave-optical evaluation of the resulting foci confirms the need for a multi-lens microscope objective as we achieve diffraction limited spots even at the limits of the working volume, see simulations shown on the top right. On the other hand, especially for two cases at the edges of the volume, the aspherical lens shows strong aberrations, mainly composed of coma, see bottom right. Here, resulting peak intensities $I_{\max}$ are reduced by one order of magnitude.

On closer inspection, one can also see the effects of our design strategy for the objective unit satisfying the Abbe sine condition.[33] In all three cases, radial symmetric intensity distributions are at hand which are marginally modulated on-axis, see top right of Fig. 3—a typical behavior for slightly spherically aberrated spots. The Herschel condition is, thus, not completely satisfied in the three cases shown. These aberrations are, however, neglectable as peak intensities and focus shapes are mainly responsibly for useful laser modifications. Here, the loss in peak intensity is smaller than 10% when working with the microscope objectives, see top right. The beam propagation factor M^2_{eff} virtually determined according to ISO1146–3[34,35] is at the diffraction limit in the geometrical focus and better than 1.4 at the working volume's edges.†

The situation with the single lens asphere is equally clear. Being optimized for the situation in the geometrical focus, see middle case depicted on the bottom right of Fig. 3, the two further cases at the edges of the working volume show strong typical coma and astigmatism aberrations.[36] The spot profiles are no longer radial symmetric and exhibit significant peak intensity losses. Thus, neither the Abbe sine, nor the Herschel condition is fulfilled.[37] This is confirmed by corresponding M^2_{eff}-parameters that amount to approximately 10. The simultaneous processing of a large working volume, $V \gtrsim (500\,\mu\mathrm{m})^3$, with multiple spots of NA > 0.2 and conventional focusing units is, thus, not recommended.

Optical properties of two designed microscope designs are listed in Table 1. These are proprietary developments that are available with the TRUMPF processing optics of the TOP product group.[2]

4. TAILORED-EDGE GLASS PROCESSING

The optical concepts from previous sections (Secs. 2 and 3) are applied to generate focus distributions for tailored-edge cleaving of non-strengthened Corning® Gorilla® glass substrates. Ultrashort laser pulses emerged from a TruMicro Series 2000 laser[38] are illuminating a central beam shaping element acting as holographic phase-only

*To be more precise, preferential directions induced by non-axisymmetric foci may be beneficial for faciliated glass separation.[1] However, laser modifications with uncontrolled crack orientation will usually result in poor edge qualities.

†The qualification of a focusing unit by means of a beam propagation ratio is of course insufficient but highly interesting from a laser technological point of view. It provides information to what extend the quality of an ideal fundamental Gaussian illumination is reduced by a non-adequate focusing. Note that the second decimal digit of the stated M^2_{eff}-parameters, cf. Fig. 3, is given only for the sake of completeness. A specification to this level of accuracy, strictly speaking, makes little sense due to numerical noise.

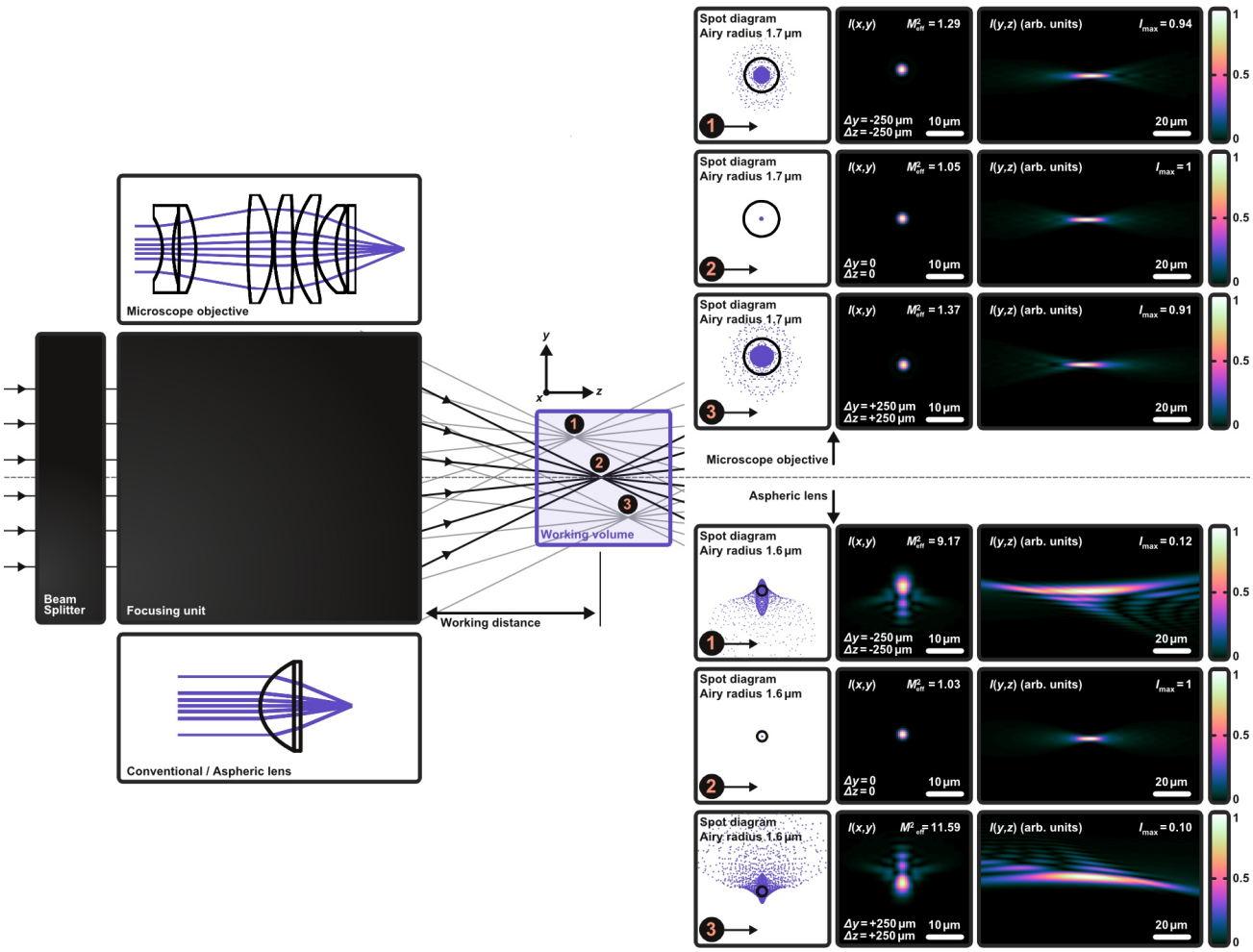

Figure 3. Comparing the focusing performance of an adapted microscope objective (top) and a conventional aspheric lens (bottom) for large volume processing with holographic 3D-beam splitters. In both cases, the effective focal length and the numerical aperture is set to $f_{\mathrm{eff}} = 10\,\mathrm{mm}$ and $\mathrm{NA} = 0.45$, respectively. The optical setup consists of the beam splitter and the focusing unit in a $2f$-like configuration[5,7] denoted by the black boxes (left). For the tailored-edge cleaving of display glasses we aim for a working volume of $\sim (500\,\mu\mathrm{m} \times 500\,\mu\mathrm{m} \times 500\,\mu\mathrm{m})$, see purple square. Here, three focusing situations are compared where three spots are independently distributed in the working volume: ❶ at $(y = -250\,\mu\mathrm{m}, z = -250\,\mu\mathrm{m})$, ❷ at $(y = 0\,, z = 0\,)$, and ❸ at $(y = 250\,\mu\mathrm{m}, z = 250\,\mu\mathrm{m})$, where case ❷ equals the geometrical focus of both focusing units. For the sake of clarity, we keep the distribution of the spots at two dimensions and set $x = 0$ for all three cases. The ray- and wave-optical evaluation of the resulting foci confirms the need for a multi-lens microscope objective as we achieve diffraction limited spots even at the limits of the working volume. The insufficient performance of the aspherical lens can be seen especially for the two large focus shifts, cases ❶ and ❸. Here, the transverse intensity profile $I\,(x, y)$ is no longer radial symmetric and the corresponding propagation $I\,(y, z)$ shows an accelerating behavior mainly due to coma aberrations. Resulting peak intensities I_{max} are reduced by one order of magnitude.

3D-beam splitter in a $2f$-like-configuration.[7] During our modification process, laser parameters were chosen to mainly generate type-III-regime modifications[12] inside the glass volume. Here, a pulse energy of $\lesssim 150\,\mu\mathrm{J}$ (for this glass type and thickness) was equally distributed to picosecond pulse trains[39,40] Feed rates were chosen to generate a modification pitch of $\sim 5\,\mu\mathrm{m}$. Please note, that the stated laser parameters of this study represent useful values and can form the basis for future investigations. However, we do not claim to have found the optimum ones. Depending on substrate geometry and material, adapted laser parameters need to be found. In addition, there will be a strong dependency on which the separation process (for example, chemical versus thermal) is actually aimed at.[41] Particularly when it comes to thermal separation with CO_2-laser radiation—

	Objective lens f10	Objective lens f20
Effective focal length	10 mm	20 mm
Magnification	20×	10×
Numerical aperture	0.42	0.33
Entrance pupil diameter	9.3 mm	14 mm
Working distance	8.5 mm	13 mm
Resolution	1.35 µm	1.79 µm
Laser damage threshold	10 J/cm^2 @ 1030 nm and 10 ns	10 J/cm^2 @ 1030 nm and 10 ns
Diffraction limited ellipsoid dimensions (half widths)		
δx	1.5 mm	1.1 mm
δy	1.5 mm	1.1 mm
δz	0.4 mm	3.4 mm

Table 1. Comparing fundamental properties of two objective designs for large working volume and large working distance applications. The "Objective lens f10" is similar to the focusing unit shown and characterized by simulations depicted in Fig. 3 (top).

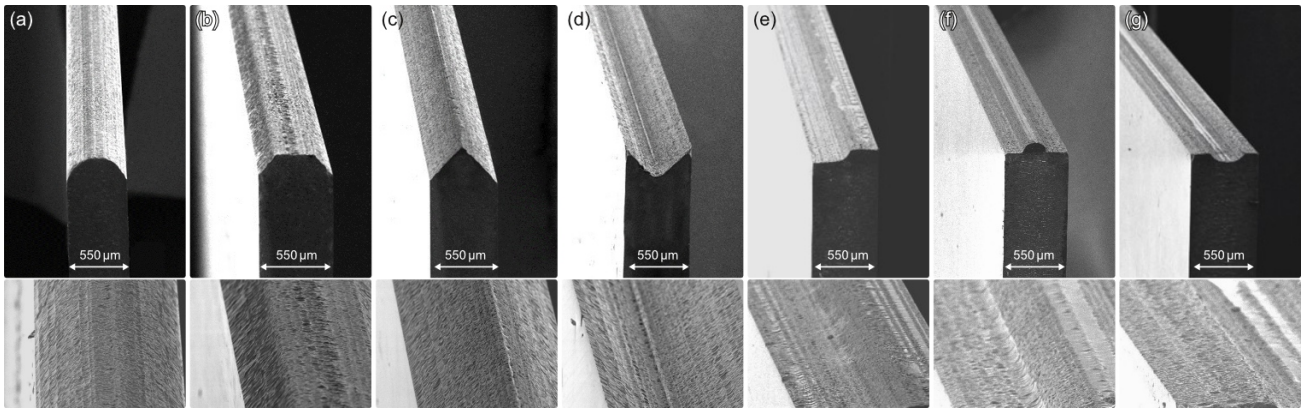

Figure 4. Menu of glass substrates with tailored-edges investigated with scanning electron microscopy. (a) C-shaped, (b) chamfered edge, (c) apex-shape, (d) inverse apex-shape, (e) (smoothed) step profile, (f) half-circle shape, (g) and inverse half-circle shape. Detailed edge images are assigned to all cases in the bottom row. In all cases, 550 µm-thick Corning® Gorilla® glass was processed with a single laser pass and subsequent chemical etching.[5] The applied focus distributions can all be seen in Fig. 2.

highly relevant from an industrial point of view—the required laser parameters will differ completely and an additional parameter study is needed.[5] Results of the first step of our tailored-edge cleaving approach, the laser modification step using volume-split spots, are analyzed in detail in Ref. 5. This also includes detailed microscope images unraveling shape, dimensions and types of the modifications.

For this second processing step, various strategies are known, for example, by applying mechanical loads[1] or by inducing thermal stresses from CO_2-laser radiation.[9] It is also well-studied that different types of laser-induced modifications can exhibit much larger etch rates than the untreated glass volume ($> 1000 : 1$).[42] This selective laser-induced etching concept enables rapid fabrication of 3D-glass structures of arbitrary shape with smallest structural features down to the 10 µm-scale.[13,42] We would like to emphasize that the actual separation concept will require adapted laser parameters and focus properties.

Our selective laser etching strategy is based on applying 30 wt.-% KOH solution to the laser-modified substrate in an ultrasonic bath operating at 80 °C.[8,41] After an etching period of < 60 min separation is achieved, made possible by the fact that the laser-induced modifications are at least partially connected by cracks.[5] Processing results are depicted in Fig. 4 where different microscope images prove a successful tailored-edge processing. This demonstrates the variety of possible edge geometries. From the perspective of protecting the glass substrate

via a shaped edge, the first two cases [Fig. 4 (a) and (b)] are of particular relevance. The cases shown in Fig. 4 (e)–(g) fulfill our motivation of substrates with enhanced auto-centering abilities. In all demonstrated cases a single-pass laser process was applied with potential to m/s-feed rates. No workpiece flipping or processing head inclination was required. The time required for chemical etching was less than one hour in all cases.

5. CONCLUSION

We have discussed the two main enabler for tailored-edge cleaving of transparent materials with ultrashort laser pulses. First, the holographic 3D-beam splitting unit required to freely distribute a large number of spots in a working volume with highest efficiencies. Secondly and equally important is an advanced large-working-volume focusing unit providing diffraction limited focus distributions along the entire edge geometry. Applying this optical concept to ultrashort laser pulses allows to deposit energy at arbitrary locations in a glass volume. The resulting material modifications exhibit a higher selective etchability which we exploit to separate the substrates by chemical means. The uniqueness of our laser optical concept is demonstrated by presenting selected processing highlights useful for edge-protecting applications such as glass samples with 45-deg chamfers. Additionally, we introduce edge contours with benefits regarding auto-centering and flush-closing. All shown samples were generated after inducing laser modifications with a single pass with the potential to m/s feed rates.

REFERENCES

1. M. Jenne, D. Flamm, K. Chen, M. Schäfer, M. Kumkar, and S. Nolte, "Facilitated glass separation by asymmetric Bessel-like beams," *Optics Express* **28**(5), pp. 6552–6564, 2020.
2. D. Flamm, J. Kleiner, M. Kaiser, F. Zimmermann, D. G. Großmann, and M. Kumkar, "Ultrafast laser cutting of transparent materials: the trend towards tailored edges and curved surfaces," in *Laser-based Micro-and Nanoprocessing XV*, **11674**, p. 116740J, International Society for Optics and Photonics, 2021.
3. S. Marjanovic, D. Andrew, P. Garrett, A. Piech, J. M. Quintal, H. Schillinger, S. Tsuda, R. S. Wagner, and A. N. Yeary, "Edge chamfering methods," Oct. 15 Oct. 15 2019. US Patent 10,442,719.
4. P. Bukieda, K. Lohr, J. Meiberg, and B. Weller, "Study on the optical quality and strength of glass edges after the grinding and polishing process," *Glass Structures & Engineering* **5**, pp. 411–428, 2020.
5. D. Flamm, M. Kaiser, M. Feil, M. Kahmann, M. Lang, J. Kleiner, and T. Hesse, "Protecting the edge: Ultrafast laser modified C-shaped glass edges," *Journal of Laser Applications* **34**(1), p. 012014, 2022.
6. D. Flamm, D. G. Grossmann, M. Jenne, F. Zimmermann, J. Kleiner, M. Kaiser, J. Hellstern, C. Tillkorn, and M. Kumkar, "Beam shaping for ultrafast materials processing," in *Laser Resonators, Microresonators, and Beam Control XXI*, **10904**, p. 109041G, International Society for Optics and Photonics, 2019.
7. D. Flamm, D. G. Grossmann, M. Sailer, M. Kaiser, F. Zimmermann, K. Chen, M. Jenne, J. Kleiner, J. Hellstern, C. Tillkorn, *et al.*, "Structured light for ultrafast laser micro-and nanoprocessing," *Optical Engineering* **60**(2), p. 025105, 2021.
8. M. Kaiser, M. Kumkar, R. Leute, J. Schmauch, R. Priester, J. Kleiner, M. Jenne, D. Flamm, and F. Zimmermann, "Selective etching of ultrafast laser modified sapphire," in *Laser Applications in Microelectronic and Optoelectronic Manufacturing (LAMOM) XXIV*, **10905**, p. 109050F, International Society for Optics and Photonics, 2019.
9. S. Nisar, L. Li, and M. Sheikh, "Laser glass cutting techniques—a review," *Journal of Laser Applications* **25**(4), p. 042010, 2013.
10. F. Lamontagne and N. Desnoyers, "New solutions in precision lens mounting," *Optical Review* **26**(4), pp. 396–405, 2019.
11. F. Lamontagne, M. Savard, N. Desnoyers, and M. Tremblay, "High accuracy lens centering using edge contact mounting," *Optical Engineering* **60**(5), p. 051212, 2021.
12. K. Itoh, W. Watanabe, S. Nolte, and C. B. Schaffer, "Ultrafast processes for bulk modification of transparent materials," *MRS bulletin* **31**(8), pp. 620–625, 2006.
13. M. Hermans, J. Gottmann, and F. Riedel, "Selective, laser-induced etching of fused silica at high scan-speeds using KOH.," *Journal of Laser Micro/Nanoengineering* **9**(2), 2014.

14. M. Kumkar, M. Kaiser, J. Kleiner, D. Grossmann, D. Flamm, K. Bergner, and S. Nolte, "Ultrafast laser processing of transparent materials supported by in-situ diagnostics," in *Laser Applications in Microelectronic and Optoelectronic Manufacturing (LAMOM) XXI*, **9735**, p. 97350P, International Society for Optics and Photonics, 2016.
15. D. Flamm, D. Grossmann, M. Kaiser, J. Kleiner, M. Kumkar, K. Bergner, and S. Nolte, "Tuning the energy deposition of ultrashort pulses inside transparent materials for laser cutting applications," *Proc. LiM* **253**, 2015.
16. G. Siviloglou, J. Broky, A. Dogariu, and D. Christodoulides, "Observation of accelerating Airy beams," *Physical Review Letters* **99**(21), p. 213901, 2007.
17. I. D. Chremmos, Z. Chen, D. N. Christodoulides, and N. K. Efremidis, "Bessel-like optical beams with arbitrary trajectories," *Optics Letters* **37**(23), pp. 5003–5005, 2012.
18. C. Ungaro and A. Liu, "Single-pass cutting of glass with a curved edge using ultrafast curving bessel beams and oblong airy beams," *Optics & Laser Technology* **144**, p. 107398, 2021.
19. D. Sohr, J. U. Thomas, and S. Skupin, "Shaping convex edges in borosilicate glass by single pass perforation with an airy beam," *Optics Letters* **46**(10), pp. 2529–2532, 2021.
20. M. Kumkar, M. Kaiser, J. Kleiner, D. Flamm, D. Grossmann, K. Bergner, F. Zimmermann, and S. Nolte, "Throughput scaling by spatial beam shaping and dynamic focusing," in *Laser Applications in Microelectronic and Optoelectronic Manufacturing (LAMOM) XXII*, **10091**, p. 100910G, International Society for Optics and Photonics, 2017.
21. F. Wyrowski, H. van Esdonk, R. J. Zuidema, S. Wadmann, and G. J. Notenboom, "Use of diffractive optics in material processing," in *Diffractive and Holographic Optics Technology*, **2152**, pp. 139–144, International Society for Optics and Photonics, 1994.
22. L. Zhu, M. Sun, M. Zhu, J. Chen, X. Gao, W. Ma, and D. Zhang, "Three-dimensional shape-controllable focal spot array created by focusing vortex beams modulated by multi-value pure-phase grating," *Optics Express* **22**(18), pp. 21354–21367, 2014.
23. M. Gu, X. Li, and Y. Cao, "Optical storage arrays: a perspective for future big data storage," *Light: Science & Applications* **3**(5), pp. e177–e177, 2014.
24. A. Jesacher and M. J. Booth, "Parallel direct laser writing in three dimensions with spatially dependent aberration correction," *Optics Express* **18**(20), pp. 21090–21099, 2010.
25. P. J. Valle and M. P. Cagigal, "Analytic design of multiple-axis, multifocal diffractive lenses," *Optics Letters* **37**(6), pp. 1121–1123, 2012.
26. D. Grossmann, M. Reininghaus, C. Kalupka, M. Kumkar, and R. Poprawe, "Transverse pump-probe microscopy of moving breakdown, filamentation and self-organized absorption in alkali aluminosilicate glass using ultrashort pulse laser," *Optics Express* **24**(20), pp. 23221–23231, 2016.
27. K. Bergner, B. Seyfarth, K. Lammers, T. Ullsperger, S. Döring, M. Heinrich, M. Kumkar, D. Flamm, A. Tünnermann, and S. Nolte, "Spatio-temporal analysis of glass volume processing using ultrashort laser pulses," *Applied Optics* **57**(16), pp. 4618–4632, 2018.
28. M. Jenne, F. Zimmermann, D. Flamm, D. Großmann, J. Kleiner, M. Kumkar, and S. Nolte, "Multi pulse pump-probe diagnostics for development of advanced transparent materials processing," *Journal of Laser Micro Nanoengineering* **13**(3), pp. 273–279, 2018.
29. K. Bergner, D. Flamm, M. Jenne, M. Kumkar, A. Tünnermann, and S. Nolte, "Time-resolved tomography of ultrafast laser-matter interaction," *Optics Express* **26**(3), pp. 2873–2883, 2018.
30. J. W. Goodman, "Introduction to Fourier optics. 3rd," *Roberts and Company Publishers* , 2005.
31. F. Ahmed, M. S. Lee, H. Sekita, T. Sumiyoshi, and M. Kamata, "Display glass cutting by femtosecond laser induced single shot periodic void array," *Applied Physics A* **93**(1), pp. 189–192, 2008.
32. S. Marjanovic, A. R. Nieber, G. A. Piech, H. Schillinger, S. Tsuda, and R. S. Wagner, "Laser cutting of display glass compositions," Dec. 26 2017. US Patent 9,850,160.
33. J. J. Braat, "Abbe sine condition and related imaging conditions in geometrical optics," in *Fifth International Topical Meeting on Education and Training in Optics*, **3190**, pp. 59–64, International Society for Optics and Photonics, 1997.

34. ISO 11146-2:2005, "Lasers and laser-related equipment—Test methods for laser beam widths, divergence angles and beam propagation ratios—Part 2: General astigmatic beams," International Organization for Standardization, 2005.
35. D. Flamm, K.-C. Hou, P. Gelszinnis, C. Schulze, S. Schröter, and M. Duparré, "Modal characterization of fiber-to-fiber coupling processes," *Optics Letters* **38**(12), pp. 2128–2130, 2013.
36. C. Schulze, A. Dudley, D. Flamm, M. Duparré, and A. Forbes, "Reconstruction of laser beam wavefronts based on mode analysis," *Applied optics* **52**(21), pp. 5312–5317, 2013.
37. J. H. Burge, C. Zhao, and M. Dubin, "Use of the abbe sine condition to quantify alignment aberrations in optical imaging systems," in *International Optical Design Conference*, p. ITuD5, Optical Society of America, 2010.
38. F. Jansen, A. Budnicki, and D. Sutter, "Pulsed lasers for industrial applications: Fiber, slab and thin-disk: Ultrafast laser technology for every application," *Laser Technik Journal* **15**(2), pp. 46–49, 2018.
39. P. R. Herman, R. Marjoribanks, and A. Oettl, "Burst-ultrafast laser machining method," Apr. 22 Apr. 22 2003. US Patent 6,552,301.
40. C. Kerse, H. Kalaycıoğlu, P. Elahi, B. Çetin, D. K. Kesim, Ö. Akçaalan, S. Yavaş, M. D. Aşık, B. Öktem, H. Hoogland, *et al.*, "Ablation-cooled material removal with ultrafast bursts of pulses," *Nature* **537**(7618), pp. 84–88, 2016.
41. H. Rave, H. Heiming, P. Szumny, M. Kaiser, J. Kleiner, and D. Flamm, "Glass tube cutting with aberration-corrected non-diffracting ultrashort laser pulses," *Optical Engineering* **60**(6), p. 065105, 2021.
42. J. Gottmann, M. Hermans, N. Repiev, and J. Ortmann, "Selective laser-induced etching of 3D precision quartz glass components for microfluidic applications—up-scaling of complexity and speed," *Micromachines* **8**(4), p. 110, 2017.